Supplementary materials.

Online methods.

Ethics and animals.

All procedures were approved by the Institutional Animal Care and Use Committees of Boston Children's Hospital, Harvard Medical School and the Université de Montréal (CDEA #19027; #19028). 8-week old male and female mice were purchased from Jackson Laboratory and housed in standard environmental conditions (12h light/dark cycle; 23^{o}C; food and water ad libitum) at facilities accredited by the Association for Assessment and Accreditation of Laboratory Animal Care.

Mouse lines.

BALB/c (Stock No: 001026), Tac1$^{-/-}$ (B6.Cg-Tac1tm1Bbm/J; Stock No: 004103), Rag1$^{-/-}$ (B6.129S7-Rag1tm1Mom/J; Stock No: 002216), Tac1^{Cre} (B6;129S-Tac1tm1.1(cre)Hze/J; Stock No: 021877), DTA$^{fl/fl}$ (B6.129P2-Gt26Sortm1(DTA)Lky/J; Stock No: 009669), ChR2$^{fl/fl}$ (B6.Cg-Gt(ROSA)26Sortm27.1(CAG-COP4*H134R/tdTomato)Hze/J; Stock No: 012567), CHAT^{ChR2}-eYFP (B6.Cg-Tg(Chat-COP4*H134R/EYFP,Slc18a3)6Gfng/J; Stock No: 014546). We used the cre/lox toolbox to genetically-engineered the various mice lines used (TRPV1$^{cre/wt}$::DTA$^{fl/wt}$, TRPV1$^{cre/wt}$::ChR2$^{fl/wt}$, Tac1$^{cre/wt}$::ChR2$^{fl/wt}$ and littermate control) by crossing male heterozygote Cre mice to female homozygous loxP mice (1). All Cre driver lines used are viable and fertile and abnormal phenotypes were not detected. Offspring were tail clipped; tissue was used to assess the presence of transgene by standard PCR, as described by Jackson Laboratory. Offspring were used at 8 weeks of age.

Asthma model

Allergic airway inflammation was studied in an ovalbumin (OVA) based model (1, 2). On day 0 and 7, mice were sensitized by a 200 µl i.p. injections of a solution containing 1 mg/ml ovalbumin (Sigma-Aldrich) and 5 mg/ml aluminum hydroxide (Sigma-Aldrich, Boston, Ma). On day 14-17 (10:00 am) mice were exposed to 6% OVA aerosol for 25min to induce airways allergic inflammation. Drugs were nebulized on day 18 (10:00 am) and outcome assessed on day 21 (10:00 am).

Drugs

QX-314(1, 3) (Charged lidocaine derivative, Tocris #2313), Carbachol (muscarinic agonist; Sigma #PHR1511), [Sar^{9}, Met(O2)^{11}]-SP (NK1R stable agonist, Tocris # 1178) were diluted fresh in sterile PBS at various concentrations. Capsaicin (TRPV1 selective agonist, Sigma #M2028) was diluted in ethanol.

ELISA

Mice were anesthetized with urethane and a 20G sterile catheter inserted longitudinally into the trachea. 2 ml of ice-cold PBS with protease inhibitor cocktail (1x Sigma Fast Protease Inhibitor (Sigma #S8820) and 10µM epoxomicin (Enzo #BMLPI127100,), was injected into the lung, harvested and underwent a 400g centrifugation (15 min; 4^{o}C) (4). The cells were discarded. Samples were processed according to instruction using commercial ELISA kit specifically designed for substance P (5) (Phoenix Pharmaceuticals; catalog number EK-064-05), Muc5B (LSBio # LS-F22247), and Muc5AC (LSBio #LS-F4842). For SP ELISAs, BALF were concentrated to a final 200 µl volume following a 3h RT SpeedVac (Thermo Scientific; SpeedVac Concentrator, SPD1010) cycle (1).

Histology

Lungs were inflated to 20 cm H_2O with 1x zinc fixative (BD Pharmigen), the trachea was ligated, and lungs stored overnight in zinc fixative (RT, mild shaking). The lungs were then washed in PBS and serially immersed in 30, 50 and 70 % Ethanol solution (20 min/each solution; RT). Tissues were embedded in paraffin, serially cut at 4µm and stained with Alcian Blue (AB; Sigma #66011500MLF) to assess goblet cell hyperplasia (6) and with Periodic Acid Schiff (PAS; Abcam #ab150680) base solution to assess mucus deposition (7). Two blinded investigators scored 384 randomized/scrambled images per condition (6 zones/slide; 4 slides/animal and 3-4 animals/group). PAS scores range from 0 (absence of goblet cells) to 4 (extensive goblets cells in large and small diameter bronchioles). AB was scored using ImageJ has relative intensity (Arbitrary Unit) over background.

Immunofluorescence

Upon harvesting, inflated lungs were post-fixed overnight in 4% para-formaldehyde, wash in PBS and cryoprotected by sequential sucrose immersion (PBS 10-30% sucrose, Overnight). Sections were then mounted in O.C.T. (Tissue-tek), and serially cut in 20 µm coronal sections with a cryostat. The sections were thaw-mounted on Fisherbrad superfrost

microscopy slides and kept at -80°C. On the day of the experiment, sections were thawed at room temperature for 10 min. Sections were washed in PBS for 5 min, blocked for 1h at room temperature (PBS, 0.1% Triton X-100, 5% BSA) and exposed to the primary antibodies (Overnight, 4°C), namely rabbit anti-mouse Muc5B (Abcam # ab87376), mouse Anti-mouse Muc5AC (Thermofisher #MA5-12178). Other antibodies tested include anti-Muc5AC (Thermofisher #MA5-12178), anti-Muc5B (Abcam #ab77995), rabbit anti-mouse Muc5B (BioS USA #bs-2414R-A555), or rabbit anti-mouse Muc5AC (Novus #NBP2-15196AF405). Sections were then washed three times in PBS (5 min), exposed to the secondary antibodies (2h, dark), washed, coverslipped with vectashield with DAPI (Vector Labs #H-1200) and observed under fluorescent microscope (Nikon. Eclipse Ti2-U).

Fluorescent *in situ* hybridization.

Inflated lungs were post-fixed overnight in 4% para-formaldehyde, wash in PBS and cryoprotected by sequential sucrose immersion (PBS 10-30% sucrose, Overnight). Sections were mounted in O.C.T. (Tissue-tek), and serially cut in 20 µm coronal sections with a cryostat. The sections were thaw-mounted on fisherbrad superfrost microscopy slides and kept at -80°C. On the day of the experiment, sections were thawed at room temperature for 10 min. Fluorescent in situ hybridization was performed as described using the RNAscope® Fluorescent Multiplex Reagent Kit (ACD Bio #320850) The primary probes used to stain Muc5B was Mm-Muc5b (ACD Bio #471991) (8) and for Muc5AC was Mm-Muc5ac-C2 (ACD Bio #448471-C2)were used as described in the instruction (9). Sections were washed in PBS (5 min), coverslipped with Vectashield with DAPI (Vector Labs #H-1200) and observed under fluorescent microscope (Nikon. Eclipse Ti2-U).

Flow cytometry

Lungs were gently lavages with PBS, harvested, digested and single cells resuspended in FACS buffer (PBS, 2% FCS, EDTA), and incubated with Fc block (0.5 mg/ml, 10 min; BD Biosciences). Cells were then stained with monoclonal antibodies (FITC anti-mouse CD45, BD Biosciences, cat no: 553079; Cy7 anti-mouse NK1R (10), Novus, NB300-119APCCY7; Dylight350 anti-mouse Muc2, Novus, NB120-11197UV; 45 min, 4°C on ice). 10^4- 10^5 $CD45^-Muc2^+$ or $CD45^-NK1R^+$ cells were isolated using a BD FACSAria™ III sorter (BD Biosciences) directly in Qiazol for subsequent qPCR measurement.

SYBR green-based quantitative real-time PCR.

RNA was extracted from whole lungs or FACS-sorted $Muc2^+$ or $NK1R^+$ lung cells using Qiazol reagent, followed by the RNeasy mini kit (Qiagen, MD). DNase I treatment (Qiagen) was used to remove genomic DNA, and complementary DNA reverse transcribed using Superscript III with random hexamers (Life Technologies). For qPCR, cDNA was subjected to 2-step thermocycling using fast SYBR green master mix (Life Technologies), and data collection performed on an Applied Biosystems 7500 machine (Life Technologies) (1). Expression levels were normalized to β-actin using the ΔΔcT method. The following primers were used: β-actin forward (TCG TAC CAC AGG CAT TGT GAT GGA) (1), β-actin reverse (TGA TGT CAC GCA CGA TTT CCC TCT) (1), Muc5b forward (CTG GCA CCT GCT CTG TGC A) (11), Muc5b reverse (CAC TGC TTT GAG GCA GTT CT) (11), Muc5AC forward (ACC ACT TTC TCC TTC TCC ACA) (11), and Muc5AC reverse (ATG GAT GTT AGC CGT CCT G) (11).

Tracheal mucus secretion

Upon euthanasia, mice tracheas were dissected and placed in ice-cold Krebs–Ringer bicarbonate buffer. The trachea was cut dorsally along its length and placed in a custom-built chamber mucosal side up so that the serosal side was bathed in ~60 µl Ringers, and the mucosal side was exposed to air (12). The luminal surface was gently cleaned with absorbent paper, dried with a stream of air, and coated with ~5 µl of mineral oil (Sigma #M5904). The luminal surface was not cleaned with absorbent paper during the experiments involving capsaicin or [Sar^9, $Met(O2)^{11}$]-SP to avoid tissue damage that might trigger nociceptive responses. Pharmacological agents (100µM Carbachol, 10µM capsaicin, 100µM QX-314, 100µM [Sar^9, $Met(O2)^{11}$]-SP) (13) were added to the serosal side and images of droplets taken at 1s intervals using a digital camera (Nikon. Ti2-U) and analyzed using ImageJ (12). Secretion volumes were calculated using the formula $V=1.3\pi r^3$, where r is the radius (12). To be included in the analysis, each droplet had to meet the following criteria: (a) a circular outline, so that it could be assumed to be spherical; (b) clear edges, to allow accurate measurement of the radius; and (c) no fusion with neighboring droplets. Viability was tested at the end of each experiment by measuring the response to carbachol, and those glands that did not respond to carbachol (<5% of total) were excluded from the analysis (12). Secretion rates were calculated as the slopes of cumulative volume vs. time plots after fitting at least three data points by linear regression (r2>0.8, rates in nanoliter per minute per gland) (12).

Vagus nerve optogenetic

Animals were deeply anesthetized (isoflurane, 1.5%–2%, Abbott Laboratory), freely breathing, and maintained at normal body temperature. The left nodose/jugular complex was surgically exposed and an optic fiber (0.39 NA fiber, Thorlabs)

was coupled to a DPSS laser light source (473 nm, 100 mW, Ultralaser) was placed 5-10 mm from the nerve (14). Focal illumination was performed beneath the ganglion and above the pharyngeal and superior laryngeal branches of the left nodose/jugular complex (14). Thirty-minute light stimulation were as follow: 3.5 ms, 5Hz, 100 mW, which give approx. 2-6 mW/mm^2 of power on the nerve, was controlled by a shutter system (Uniblitz) (15).

Statistics

Data expressed as mean ± S.E.M. Statistical significance determined by two-tail unpaired Student's t-test. P values less than 0.05 were considered significant. Numbers of animals are defined in figures.

Online references.

1. Talbot S, Abdulnour RE, Burkett PR, Lee S, Cronin SJ, Pascal MA, et al. Silencing Nociceptor Neurons Reduces Allergic Airway Inflammation. Neuron. 2015;87(2):341-54.

2. Haworth O, Cernadas M, Yang R, Serhan CN, Levy BD. Resolvin E1 regulates interleukin 23, interferon-gamma and lipoxin A4 to promote the resolution of allergic airway inflammation. Nat Immunol. 2008;9(8):873-9.

3. Binshtok AM, Bean BP, Woolf CJ. Inhibition of nociceptors by TRPV1-mediated entry of impermeant sodium channel blockers. Nature. 2007;449(7162):607-10.

4. Krause T, Rockendorf N, Gaede KI, Ramaker K, Sinnecker H, Frey A. Validation of antibody reagents for mucin analysis in chronic inflammatory airway diseases. MAbs. 2017;9(2):333-41.

5. Herberth G, Daegelmann C, Weber A, Roder S, Giese T, Kramer U, et al. Association of neuropeptides with Th1/Th2 balance and allergic sensitization in children. Clin Exp Allergy. 2006;36(11):1408-16.

6. Temann UA, Geba GP, Rankin JA, Flavell RA. Expression of interleukin 9 in the lungs of transgenic mice causes airway inflammation, mast cell hyperplasia, and bronchial hyperresponsiveness. J Exp Med. 1998;188(7):1307-20.

7. Gu W, Zhang X, Yan Y, Wang Y, Huang L, Wang M, et al. B7-H3 participates in the development of Asthma by augmentation of the inflammatory response independent of TLR2 pathway. Sci Rep. 2017;7:40398.

8. Chen G, Sun L, Kato T, Okuda K, Martino MB, Abzhanova A, et al. IL-1beta dominates the promucin secretory cytokine profile in cystic fibrosis. J Clin Invest. 2019;129(10):4433-50.

9. Han S, Fink J, Jorg DJ, Lee E, Yum MK, Chatzeli L, et al. Defining the Identity and Dynamics of Adult Gastric Isthmus Stem Cells. Cell Stem Cell. 2019;25(3):342-56 e7.

10. Zhou Y, Wang M, Tong Y, Liu X, Zhang L, Dong D, et al. miR-206 Promotes Cancer Progression by Targeting Full-Length Neurokinin-1 Receptor in Breast Cancer. Technol Cancer Res Treat. 2019;18:1533033819875168.

11. Ehre C, Worthington EN, Liesman RM, Grubb BR, Barbier D, O'Neal WK, et al. Overexpressing mouse model demonstrates the protective role of Muc5ac in the lungs. Proc Natl Acad Sci U S A. 2012;109(41):16528-33.

12. Ianowski JP, Choi JY, Wine JJ, Hanrahan JW. Substance P stimulates CFTR-dependent fluid secretion by mouse tracheal submucosal glands. Pflugers Arch. 2008;457(2):529-37.

13. Talbot S, Chahmi E, Dias JP, Couture R. Key role for spinal dorsal horn microglial kinin B1 receptor in early diabetic pain neuropathy. J Neuroinflammation. 2010;7(1):36.

14. Chang RB, Strochlic DE, Williams EK, Umans BD, Liberles SD. Vagal Sensory Neuron Subtypes that Differentially Control Breathing. Cell. 2015;161(3):622-33.

15. Browne LE, Latremoliere A, Lehnert BP, Grantham A, Ward C, Alexandre C, et al. Time-Resolved Fast Mammalian Behavior Reveals the Complexity of Protective Pain Responses. Cell Rep. 2017;20(1):89-98.

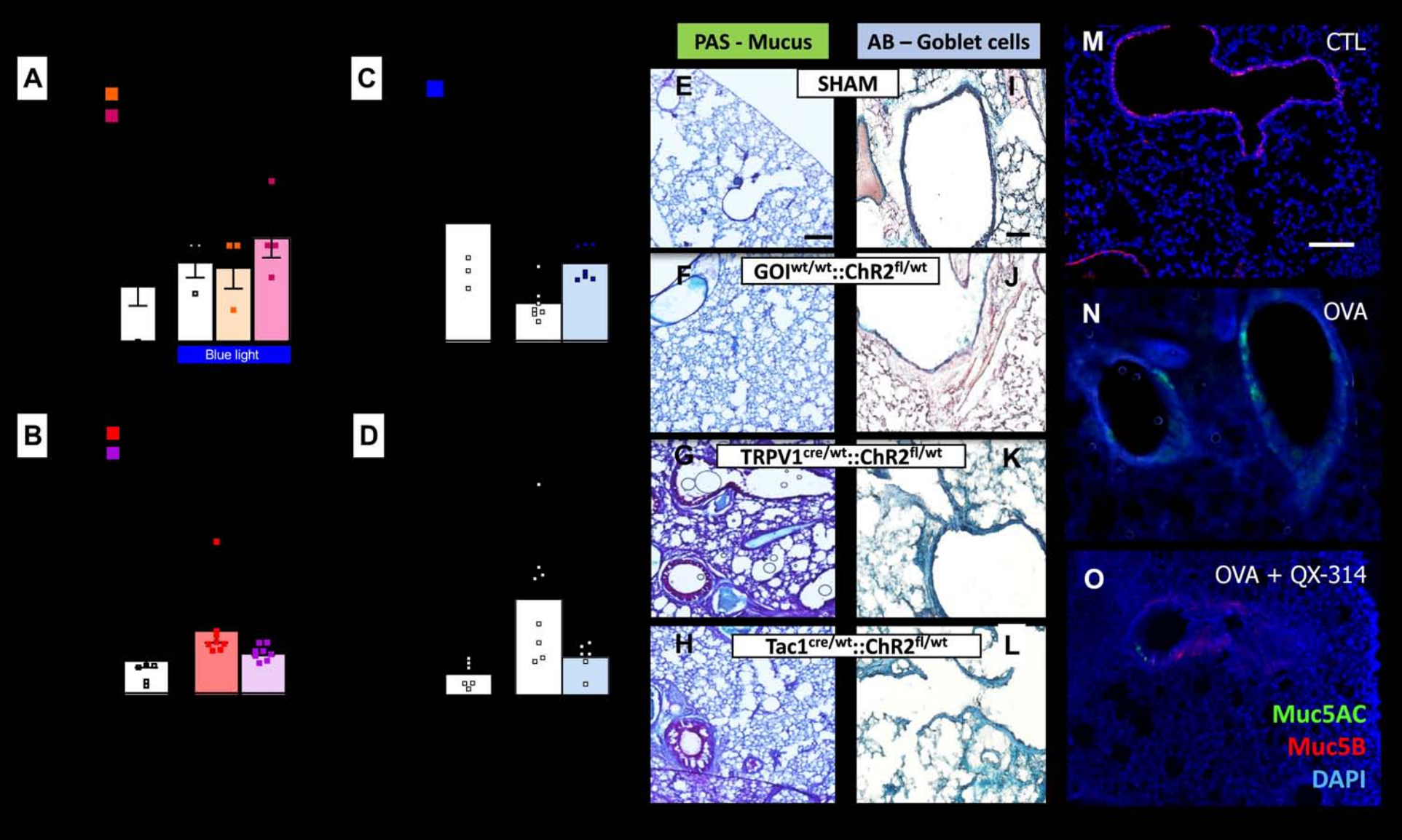
A
B
C
D
Blue light
PAS - Mucus
AB – Goblet cells
E
SHAM
I
F
GOI$^{wt/wt}$::ChR2$^{fl/wt}$
J
G
TRPV1$^{cre/wt}$::ChR2$^{fl/wt}$
K
H
Tac1$^{cre/wt}$::ChR2$^{fl/wt}$
L
M
CTL
N
OVA
O
OVA + QX-314
Muc5AC
Muc5B
DAPI

A
B
C
D
PAS - Mucus
In situ – Muc5AC
E
F
G
H
I
J
K
L
M
N
DAPI
Muc5AC
CTL
WT + OVA
DTA fl/wt + OVA
SP-/- + OVA
DTA fl/wt + OVA + SP

Supplementary figure legends.

Supplementary figure 1: Silencing sensory neuron neurons rescues allergen-mediated mucin imbalance. Optogenetic-stimulated (473nM, 5 Hz, 3.5 ms, 30 min, 100 mW) $TRPV1^{cre/wt}$::$ChR2^{fl/wt}$, $Tac1^{cre/wt}$::$ChR2^{fl/wt}$ and littermate control mice did not affect goblet cell hyperplasia (A). An acute capsaicin (1 uM, i.n.; B) or repeated allergen-challenges (C, D) increased airway goblet cell transcript expression (B, C) or BALF levels (D) of Muc5AC over Muc5B, these effects were reversed by sensory neuron silencing using QX-314 (100 uM; B-D). SHAM (E, I), and optogenetic-stimulated littermate control (F, J), $TRPV1^{cre/wt}$::$ChR2^{fl/wt}$ (G, K) and $Tac1^{cre/wt}$::$ChR2^{fl/wt}$ (H, L) mice lung section stained for mucus deposition (PAS, purple; E-H; Scale 100 µm) and goblet cell hyperplasia (AB, blue; I-L; Scale 30 µm). DAPI-stained cell nucleus (blue), Muc5B (red), Muc5AC (green)-stained sections of naïve (M) and OVA-exposed (N, O) lungs treated with saline (M, N) or QX-314 (100 µM; O). Scale 30 µm. Mean ± S.E.M; Two-tailed unpaired Student's t-test.

Supplementary figure 2: Sensory neuron silencing blocks SP release. OVA-challenge increased BALF Substance P, an effect prevented by sensory neuron silencing with QX-314 (100 µM, nebulized) (A). The TRPV1 agonist capsaicin (10 µM, 5 min), the stable NK-1R agonist [Sar^{9}-Met-$(O2)^{11}$]-SP (100 µM, 5 min) and carbachol (100 µM, 30 min) induced mucus secretion from OVA-challenged mice trachea (B-C). Capsaicin had no effect when administered to $TRPV1^{cre/wt}$::$DTA^{fl/wt}$ or $Tac1^{-/-}$ mice (B). QX-314 co-treatment do not impact carbachol (100 µM, 30 min) induced mucus secretion from OVA-challenged mice trachea (C). OVA-challenge increased lung $NK\text{-}1R^{+}$ goblet cells Muc5AC/Muc5B ratio, an effect prevented by sensory neuron silencing with QX-314 and absent in $Tac1^{-/-}$ mice (D). Representative periodic acid–Schiff (purple, E-I) and *Muc5ac in situ* hybridization staining (red, J-N) of naïve (E, J), OVA-challenge littermate control (F, K), OVA-challenge $TRPV1^{cre/wt}$::$DTA^{fl/wt}$ (G, L), OVA-challenged $Tac1^{-/-}$ (H, M) or OVA-challenge $TRPV1^{cre/wt}$::$DTA^{fl/wt}$ + [Sar^{9}, $Met(O2)^{11}$]-SP (I, N) mice lung. Scale of 70 µm (I) and 30 µm (N), respectively. Mean ± S.E.M; Two-tailed unpaired Student's t-test.